Astrochemistry and Solid-State Physics

WHAT LIES HIDDEN IN THE ISO ARCHIVE ON SOLID-STATE DUST FEATURES?

Christine Joblin

Centre d'Etude Spatiale des Rayonnements, CNRS et Université Paul Sabatier, BP 4346, 31028 Toulouse Cedex 04, France

ABSTRACT

The Infrared Space Observatory has revolutionized the study of solid-state interstellar matter whether this refers to molecular ices, carbonaceous dust or oxides (silicates and others). Promising studies have been initiated on the formation and processing of dust in the cycle of interstellar matter. Dust features are also becoming a powerful and, in a way, unique tool to quantify the evolutionary stage of astronomical objects. This paper provides a short overview of this rich field, underlining the importance of a full, thoughtful and organised exploitation of the ISO Data Archive in close connection with a large field of activities: laboratory experiments, theory and radiative transfer modelling.

Key words: Infrared Space Observatory – dust : ices, polycyclic aromatic hydrocarbons, silicates – interstellar and circumstellar matter – infrared, abundances, band profile – laboratory experiments, modelling

1. INTRODUCTION

The study of solid interstellar matter is certainly the field which takes the largest advantage of the spectroscopic and imagery capabilities of the four instruments on board the European Infrared Space Observatory (ISO): the camera CAM, the short- and long-wavelength spectrometers SWS and LWS, and the photometer PHT. The broad infrared spectral range covered by ISO is particularly well suited to reveal the chemical nature of dust. Other information derived from the data is abundances, constrained by elemental depletions and the characterisation of the local physical and chemical conditions. The goal is to establish dust features as a tool for astronomers to classify objects. The ISO view of a large variety of places in the Galaxy also makes it possible to study the cycling of dust in the interstellar medium from its formation to its destruction sites and through its evolution by photophysical and chemical processing.

The success of the ISO data for studies on solid-state matter relies on several aspects. The large and continuous spectral coverage (2.5 - 196 μm) allows a budget to be drawn of the various dust features within a given object and therefore provides strong constraints for physical and chemical modelling. The spectral resolution of the instrument is well-adapted for solid-state features (R~200-2000) and the wealth of available data makes possible a classification of objects as a function

of the observed features. However, the success of the observations would only be partial without the support from laboratory experiments to study the optical constants of interstellar dust analogues, the formation of these species and their further evolution under various chemical and physical processes: UV irradiation, energetic ion bombardment, gas or dust collisions (sticking and coagulation processes taking place in molecular clouds, shattering in shocks). Radiative transfer modelling appears also to be essential in deriving quantitative information from the observed spectra. These aspects are illustrated in the following, using three classes of dust that probe different types of environments: ices in molecular (cold and dense) clouds, polycyclic aromatic hydrocarbons and related species in photo-dissociation regions and finally, crystalline silicates as well as some metallic oxides which are mostly (but not only) found in circumstellar environments. In each case, emphasis is given on the perspectives provided by the exploitation of the ISO Data Archive.

2. MOLECULAR ICES

ISO enables a clear detection of rather simple molecules in ices (CO, CO_2, CH_4, H_2O...) whereas the observation of these molecules with ground-based telescopes is impossible in most cases. For example, large amounts of interstellar CO_2 (de Graauw et al. 1996) and CH_4 (Boogert et al. 1996) were detected with ISO. Such detection is only possible in the vibrational range of their spectrum since these molecules do not have allowed transitions in the radio. The measurement of the infrared absorption spectrum of ices requires a strong background source, which naturally induces some bias in the selection of the probed regions towards the environment of protostars. For instance, d'Hendecourt et al. (1996) report very strong ice features in RAFGL 7009S and provide a nice comparison of the observed spectrum with the laboratory spectrum of UV photolysed ices (cf. Fig. 1). A detailed study of the positions and shapes of the bands can provide information on the composition of ices as well as on the physical conditions which they have experienced. For instance, the bending mode of CO_2 at 15.2 μm was observed to be split in the environment of protostars (Ehrenfreund et al. 1998; Gerakines et al. 1999). On the basis of careful laboratory work (Ehrenfreund et al. 1998; Dartois et al. 1999a) this splitting was attributed to the combined effect of the presence of methanol (CH_3OH) which forms molecular complexes with CO_2 and of thermal processing of ices in the environment of protostars (cf. Fig. 2). Solid-state

methanol was subsequently detected towards RAFGL 7009S and W 33A in ground-based observations (Dartois et al. 1999b).
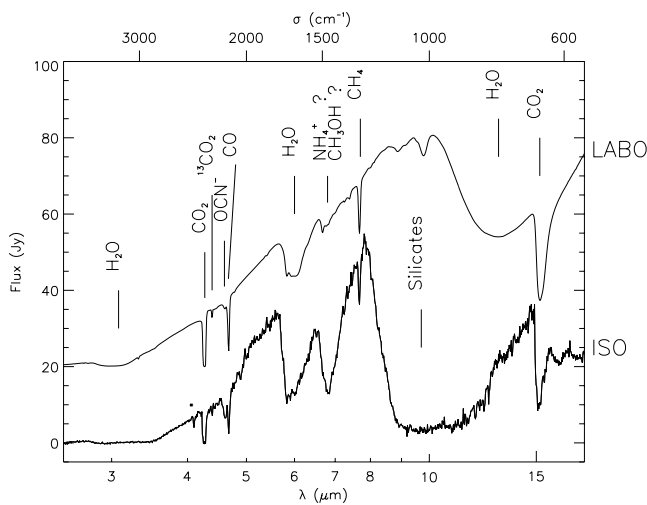

Figure 1. The 2.5-18 μm SWS spectrum measured towards the massive protostar RAFGL 7009S (bottom spectrum) compared with the laboratory spectrum of an ice mixture of H_2O:CO:CH_4:NH_3:O_2 ∼ 10:2:1:1:1 deposited at 10 K and submitted to UV photolysis. From Dartois et al. (1999c).

Different perspectives concerning the study of ices using the ISO database can be listed. There is a general interest in characterizing gas-grain interactions to evaluate the role that grains play in building molecular complexity. Various aspects have to be considered including surface chemistry, sticking and desorption processes. In this field, multi-wavelength studies of solid-state and gas-phase features, using ISO data and complementary ground-based observations, have to be encouraged in order to provide a comprehensive view of the nature and morphology of the observed region. This is nicely illustrated for the protostars RAFGL 7009S (Dartois et al. 1998, 2000) and Elias 29 (Boogert et al. 2002). Energetic processes that can trigger desorption such as cosmic rays or chemical reactions have to be further explored in the laboratory and in space. The question of how molecules are formed in interstellar ices is also still open. Are they produced by irradiation of ices or by grain surface reactions? For instance CO_2 can be formed by UV irradiation of H_2O:CO ices (d'Hendecourt et al. 1986) or by grain surface reactions between CO and O (Tielens & Hagen 1982). To disentangle the two formation mechanisms, it is necessary to search for species that are unambiguously products of energetic processing but these are likely to give rise to minor features in the IR spectra. Species that are intermediates in low-temperature solid chemistry have also to be searched for. This requires dedicated laboratory experiments which couple IR spectroscopy to mass spectrometry (Hiraoka et al. 1998) or even to more sensitive techniques such as electron paramagnetic resonance spectrometry (Zhitnikov & Dmitriev 2002). Recent experiments (Hiraoka et al. 2002) show that the production of CH_3OH in a CO solid matrix submitted to H atoms is a slow process in the conditions of cold dark clouds but becomes much faster when submitted to UV light irradiation.

Another important prospect is how to use ices as tracers of the evolution of astronomical objects including comets (Ehrenfreund 1999). Evidence is now given that thermal processing of ices can be traced by the variations of the CO_2 band profiles (especially the 15.2 μm band but also the 4.27 μm band according to Boogert et al. (2000) and references therein), as well as by the presence of complex molecules such as CH_3OH in solid state. A recent study of the SWS spectrum of young stellar objects of low-to-intermediate mass (Nummelin et al. 2001) confirms this assignment. The ISO archive allows for systematic studies on the distribution of various ices as a function of the object types. These studies have however often to be coupled with radiative transfer modelling. Also one has to consider that in interstellar space, ices are not found as infinite films but as mantles at the surface of grains of various sizes and shapes. Scattering calculations have therefore to be performed using optical constants derived from laboratory measurements (cf. for instance Ehrenfreund et al. 1997). These calculations are not straightforward and must be addressed with great caution.
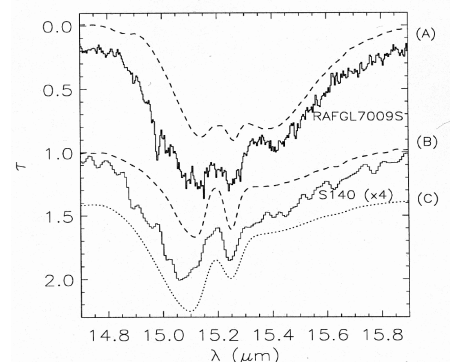

Figure 2. Infrared bending mode of CO_2 measured by the spectrometer SWS of ISO towards the massive protostars RAFGL 7009S and S 140 compared with laboratory spectra of H_2O:CO_2:CH_3OH (1.3:1:1) mixtures deposited at 10 K and warmed up to 80-90 K in (A) and 110-120 K in (B). Case (C) is comparable to (B) except that CH_3CH_2OH was deposited in the ice mixture instead of CH_3OH. From Dartois et al. (1999a).

3. PAHS AND CARBON DUST

The mid-infrared spectrum comprises a rich set of infrared emission features which are well-observed in regions where UV photons are available such as reflection nebulae, planetary nebulae, HII regions (cf. Fig. 3), high-latitude cirrus and external galaxies. Amongst the observed features are the well-known infrared bands at 3.3, 6.2, "7.7", 8.6, 11.3 and 12.7 μm which are called aromatic infrared bands (AIBs) in the following. The band at "7.7" μm consists of several components, the two main components being located at 7.6 and 7.8 μm (see Figs. 3 and 5).

In some objects the bands lie on the top of broader features and continua (cf. Fig. 3) but both types of spectral features (band and continua) are not associated to each other. The best assignment for the AIBs is polycyclic aromatic hydrocarbons (PAHs; Léger & Puget 1984; Allamandola et al. 1985) although work has still to be done to identify the involved species.
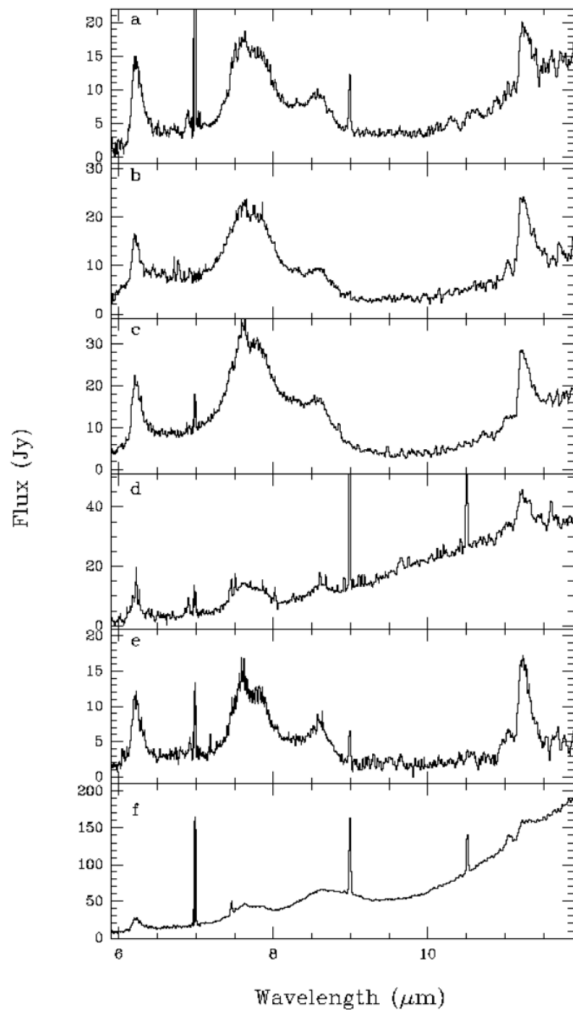

Figure 3. The ISO SWS spectra of six compact HII regions illustrating several emission features: the aromatic infrared bands at 6.2, "7.7" (7.6, 7.8), 8.6 and 11.3 μm, some continuum or broad-shaped emission as well as sharp ionic lines. From Roelfsema et al. (1996).

It was not for ISO to discover the mid-IR emission features but it did increase significantly the number of observed regions as well as the quality of the data making a quantitative analysis possible. The intensities of the AIBs were found to be proportional to the intensity of the UV radiation field (Boulanger et al. 1998). This is consistent with an excitation mechanism driven by the absorption of single UV photons. The IR emission spectrum of gas-phase PAHs following the excitation by

UV photons has been recorded in the laboratory (Cook et al. 1998 and references therein). These measurements as well as measurements on thermally excited PAHs have shown that the spectral characteristics of the IR bands (position and width) depend on the internal vibrational energy. The observed emission profiles hence result from the integration of all the individual contributions during the cooling of the molecule (cf. Fig. 4). Pech et al. (2002) showed that intramolecular effects can account for most of the profiles of the 6.2 and 11.3 μm bands observed in the planetary nebula IRAS 21282+5050. This leaves very little room for molecular diversity, suggesting the presence of only a few species or of a family of species with close spectral characteristics. If this is true then there might be some active selection either in the formation process or during further processing (for instance photodissociation induced by UV photons) in the regions where the AIBs are observed. A similar study by Verstraete et al. (2001) led to the conclusion that small PAHs are efficiently photodissociated in harsher radiation fields, implying similar AIBs in photodissociation regions illuminated by stars whose effective temperature varies from 23000 to 45000 K. Peeters et al. (2002) studied the 6-9 μm spectrum of a much larger set of objects and report variations of the band position and profile from source to source, which apparently revealed some processing of the emitting population.
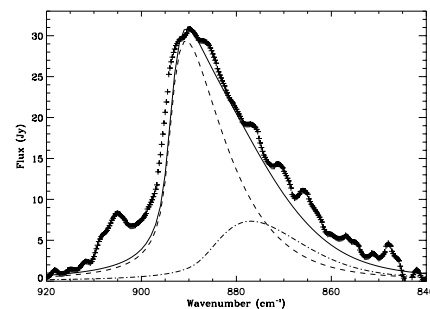

Figure 4. The 11.3 μm band profile (solid line) calculated for a size distribution of PAH-like species and compared with the band observed by ISO SWS in the planetary nebula IRAS 21282+5050 (crosses). The contribution from the fundamental and the hot bands are given by the dashed line and the dot-dashed line respectively. From Pech et al. (2002).

The question of the formation of PAHs in the interstellar medium is also a very challenging one. Models have been developed to describe the formation of PAHs in the outflows of carbon-rich AGB stars in a chemical kinetic scheme based on soot formation in hydrocarbon flames (Frenklach & Feigelson 1989; Cherchneff et al. 1992). However, none of the first products of the isomerization of acetylene C_2H_2 up to the first aromatic cycle C_6H_6 were found in the ISO spectrum of the prototype AGB star IRC +10216 (Cernicharo et al. 2001). On the other hand, the authors detected C_4H_2, C_6H_2 and C_6H_6 in the proto-planetary nebula CRL 618, suggesting that energetic processes such as UV irradiation or shocks play an im-
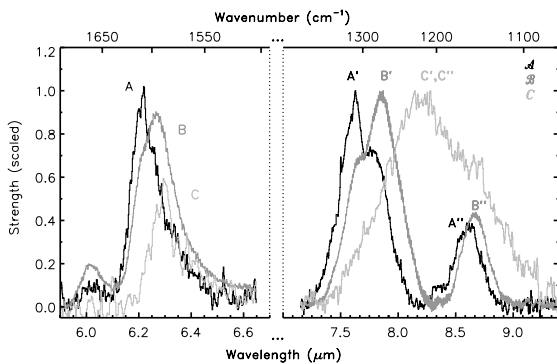
Figure 5. Variation of the emission features observed in the 6-9 μm range. Class A represents the more usual AIBs observed for instance in reflection nebulae whereas class C is representative of evolved (post-AGB) stars. Class B is an intermediate spectrum observed in isolated Herbig Ae/Be stars and in planetary nebulae. This classification underlines the importance of the processing of carbon dust from its formation sites to the interstellar medium. From Peeters et al. (2002).

portant role in the chemistry of these species. Another possibility is that homogeneous nucleation of PAHs is relatively unimportant and that most PAHs grow at the surface of heterogeneous grains, being later desorbed by UV radiation (Cadwell et al. 1994). Several papers based on ISO observations give evidence for chemical and physical evolution of carbonaceous dust. The compilation made by Peeters et al. (2002) shows that the 6-9 μm spectrum of evolved stars (post-AGB) differs from the typical AIB spectrum observed for instance in reflection nebulae (Fig. 5). Kwok et al. (1999) reported other features at longer wavelengths which are specific to the proto-planetary nebulae but disappear in the more evolved stage of planetary nebulae, revealing chemical and physical evolution of carbonaceous dust in the presence of a significant flux of UV photons. Other clues came from spectro-imaging studies of photodissociation regions (PDRs) with ISOCAM. Joblin et al. (2000) discuss how the study of the variations of the mid-IR emission features can be addressed either by considering a large sample of different objects or by studying spatial variations within extended regions. Using the capabilities of ISOCAM, Boissel et al. (2001) and Abergel et al. (2002) applied the second approach to PDRs and propose the presence of a population of very small grains which appear to produce PAHs, most likely by photoevaporation. A first spectrum for this population of small grains was derived by Boissel et al. (2001) by applying a singular value decomposition analysis to the ISOCAM data. Completing these few studies by a further exploitation of the ISO Data Archive would surely tell a lot about the origin of PAHs and their role in carbon chemistry.

Another way to progress in the identification of interstellar PAHs is to search for features at wavelengths longer than those of the AIBs. PAHs have IR modes which can fall down to the submillimetre range (Moutou et al. 1996, Joblin et al. 2002). The detection of such bands is likely to be difficult due to a combined effect of low intensity and of significant emission

from dust. However, it would be very valuable to identify interstellar PAH species. The detection of only one band at 16.4 μm has been reported so far (Van Kerckhoven et al. 2000; Moutou et al. 2000).

4. CRYSTALLINE SILICATES

Before ISO, the presence of amorphous silicates was inferred to account for broad bands at 9.7 and 18 μm. One of the great revolutions of ISO was to reveal the presence of crystalline silicates in comets (Crovisier et al. 1997), in circumstellar disks around young pre-main-sequence stars (cf. Fig. 6 and Waelkens et al. 1996) and in dust shells and disks around evolved oxygen-rich stars (Waters et al. 1996; Waters et al. 1998a; Sylvester et al. 1999; Molster et al. 2002a). The crystalline silicates give rise to sharp features between 20 and 45 μm, the majority of the observed features being due to olivines ($Mg_{2x}Fe_{(2-2x)}SiO_4$) and pyroxenes ($Mg_xFe_{(1-x)}SiO_3$ ($0 \leq x \leq 1$) with x close to unity. Astronomical crystalline silicates are therefore Mg-rich and Fe-poor olivines and pyroxenes. It is also possible that some of the observed features, especially those shortward of 30 μm, are due to other types of oxides. The study of all these new features opens, thanks to ISO, new perspectives giving rise to the field of "astromineralogy".
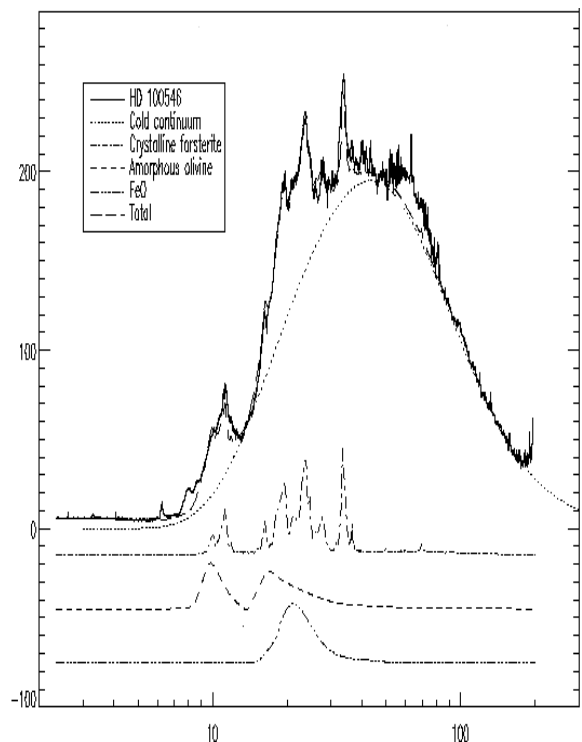

Figure 6. The full SWS-LWS spectrum of the Herbig Ae/Be star HD 100546 exhibiting numerous features attributed to crystalline silicates in particular crystalline fosterite (Mg_2SiO_4) as determined from laboratory spectra (Koike et al. 1993). The flux (in Jy) is plotted versus the wavelength (in μm). From Malfait et al. (1998).

The peak positions and shapes of the crystalline silicate features are affected by different characteristics of the grains: their composition, temperature, size and shape, and also their micro-structure such as their degree of crystallinity and porosity (cf. for instance Molster et al. 2002b). Laboratory studies provide optical properties as a function of composition (Koike et al. 1993; Jäger et al. 1998; Koike et al. 2000) and temperature (Henning & Mutschke 1997; Bowey et al. 2001; Chihara et al. 2001). For instance, the band positions were found to shift to larger wavelengths with increasing iron content (Fabian et al. 2001; Chihara et al. 2002). In order to determine quantitatively the composition and structure of dust in circumstellar environments, laboratory data has often to be used in the frame of radiative transfer models. Furthermore, one has to consider a grain shape and size distribution to derive absorption and scattering efficiencies from the optical constants. Using spheres or a continuous distribution of ellipsoids can lead to significant differences (for illustration, see Fig. 3 from Molster et al. 2002b).

Calculations were performed by several authors to study the composition and abundance of amorphous and crystalline silicates in different objects (Demyk et al. 1999; Kemper et al. 2002; Molster et al. 2002c). These studies can also reveal the presence of grains whose contribution in the spectrum is not obvious. For instance, the presence of metallic iron grains was proposed by Bouwman et al. (2000) and Kemper et al (2002), and the presence of aluminium oxides and aluminosilicates by Demyk et al. (1999). Another important result by Kemper et al. (2001) was to show that the dust shells of low mass-loss rate AGB stars could contain a significant fraction of crystalline silicates without giving any specific sharp spectral signatures. This can be accounted by a temperature effect related to the low optical thickness of the envelope, contrary to the case of high mass-loss stars.

Studies on the composition, abundance, grain size and shape are fundamental to constrain the nucleation and condensation processes of silicates, other oxides and metallic grains. What are the seeds that lead to further growth of these grains? Are they Al_2O_3, TiO_2, TiC, MgO or Fe cores? For instance, the condensation sequence of silicates at thermodynamic equilibrium starts with Al_2O_3 (cf. Tielens et al. 1998). How far can the thermodynamic sequence be obeyed in the condensation process? The information derived from the observations can give some clues to these questions (see Tielens et al. 1998) in comparison with the results of condensation experiments (Tsuchiyama 1998) and theory. There is a need to search for weak features in the ISO archive that could trace the condensation sequence(s). It is also important to characterize the size and temperature of grains and diagnostics have to be searched for. Recently, it has been shown that the 69 μm band of fosterite can be used as a dust temperature indicator (Bowey et al. 2002; Molster et al. 2002c). Finally, important information on circumstellar grains can be obtained from the analysis of interplanetary dust particles and primitive meteorites (Bernatowicz et al. 1996; Bradley et al. 1999).

The evolution of crystalline silicates is also of great interest in studying the physics and chemistry of dust in various environments. For instance, the presence of crystalline silicates both in the outflows of evolved stars and in protostellar disks has to be reconciled with their apparent absence in the interstellar medium. Crystalline silicates are also found in primitive solar system matter (Bradley et al. 1999) and are therefore potential building blocks for planetary formation.

The question of the processing of silicates has motivated laboratory simulations. Amorphization was found to occur when crystalline silicates are irradiated by He^+ ions at energies of 4 and 10 keV which simulate ion implantation in supernova shocks (cf. Fig. 7 and Demyk et al. 2001). These results provide a plausible explanation for the predominance of amorphous silicates in the interstellar medium (Li & Draine 2001). Crystallisation was obtained by annealing (Brucato et al. 1999) but activation energies were derived which are too high to account for crystallisation of silicates in cometary environments. There is therefore a need to search for alternative mechanisms. Some clues are likely to be found by a close examination of the ISO archive and by encompassing a large sample of objects to trace the evolution of silicates from their production sites to their incorporation into planetary systems.
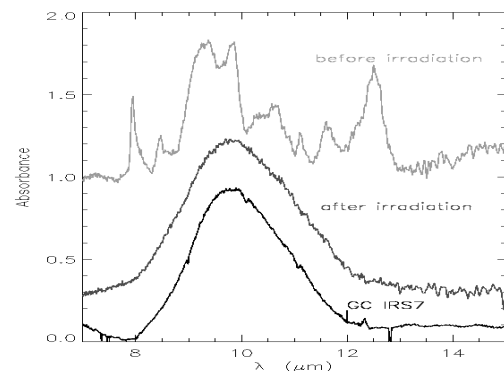

Figure 7. Comparison of the stretching mode of amorphous silicates observed towards the Galactic Center (lower spectrum) with the spectrum of crystalline enstatite before (upper spectrum) and after (middle spectrum) irradiation with a flux of 10^{18} He^+ ions/cm^2 at 10 keV. This irradiation simulates the ionic irradiation experienced by grains during supernova shock propagation in the interstellar medium. The laboratory spectra clearly show that it leads to amorphisation of the grain structure. From K. Demyk (private communication)

The discovery of crystalline silicates by ISO has also allowed a great step forward in quantitative studies of circumstellar environments. Molster et al. (2002a) have made an inventory of the bands present in the spectra of evolved stars probing the evolution from the asymptotic giant branch (AGB) to the planetary nebula phase. The results show spectral variations which allow discrimination between "disk" sources and "outflow" sources. Some evolved objects were found to have a rich spectrum with signatures of both C-rich and O-rich chemistry. This is the case of the planetary nebula NGC 6302 (Mol-

ster et al. 2001a) and of the post-AGB stars IRAS 09425-6040 (Molster et al. 2001b) and HD 44179 (the Red Rectangle; Waters et al. 1998b). In these objects, complementary observations at high spatial resolution could allow the various contributions to be separated (cf. Waters et al. 1998b). Another field of great interest is that of disks surrounding young pre-main-sequence stars which can give important clues in the understanding of planetary system formation (Waelkens et al. 1996). Interestingly, the spectrum of the Herbig Ae/Be (HAeBe) star HD 100546 (Fig. 6) reveals a high abundance of crystalline silicates whose composition is similar to that observed in comet Hale-Bopp (Crovisier et al. 1997). Evidence for dust coagulation and growth in the disks of HAeBe stars was given by Bouwman et al. (2000) and by Meeus et al. (2001).

5. CONCLUSION

The capabilities of the ISO instruments have allowed to make a great step forward in the study of interstellar dust and its use as a tracer of the physical and chemical evolution of astronomical objects. In early February 1998, a workshop was held in Les Houches on the topic: "Solid state matter : the ISO revolution". This success was put in perspective at the end of the preface of the book (d'Hendecourt et al. 1999): "However, the final ISO database, after 30 months of successful operations, remains largely untouched today. There can be no doubt that the final picture of interstellar and circumstellar dust to emerge from this database will reinforce the true originality provided by the technological success of the Infrared Space Observatory". A few years later, we can claim that great progress has been achieved but efforts have still to be maintained and supported for a decade or more.

REFERENCES

Abergel, A., Bernard, J. P., Boulanger, F., et al., 2002, A&A, 389, 239

Allamandola, L. J., Tielens, A. G. G. M., & Barker, J. R., 1985, ApJ, 290, L25

Bernatowicz, T. J., Cowsik, R., Gibbons, P. C., et al., 1996, ApJ, 472, 760

Boissel, P., Joblin, C., & Pernot, P., 2001, A&A, 373, L5

Boogert, A. C. A., Schutte, W. A., Tielens, A. G. G. M., & Whittet, D. C. B., 1996, A&A, 315, L377

Boogert, A. C. A., Ehrenfreund, P., Gerakines, P. A., et al., 2000, A&A, 353, 349

Boogert, A. C. A., Hogerheijde, M. R., Ceccarelli, C., et al., 2002, ApJ, 570, 708

Boulanger, F., Abergel, A., Bernard, J.-P., et al., 1998, in ASP Conf. Ser. 132, Star Formation with the Infrared Space Observatory, ed. J. Yun & R. Liseau, ASP Pub., San Francisco, 15

Bouwman, J., de Koter, A., van den Ancker, M. E., & Waters, L. B. F. M., 2000, A&A, 360, 213

Bowey, J. E., Lee, C., Tucker, C., et al., 2001, MNRAS, 325, 886

Bowey, J. E., Barlow, M. J., Molster, F. J., et al., 2002, MNRAS, 331, L1

Bradley, J. P., Snow, T. P., Brownlee, D. E. & Hanner, M. S., 1999, in Les Houches Ser. 11, Solid Interstellar Matter: The ISO Revolution, ed. L. d'Hendecourt , C. Joblin & A. Jones, EDP Sciences, Les Ulis, 297

Brucato, J. R., Colangeli, L., Mennella, V., Palumbo, P., Bussoletti, E., 1999, A&A, 348, 1012

Cadwell, B. J., Wang, H.; Feigelson, E. D., & Frenklach, M., 1994, ApJ, 429, 285

Cernicharo, J., Heras, A. M., Tielens, A. G. G. M., et al., 2001, ApJ, 546, L123

Cherchneff, I., Barker, J. R., & Tielens, A. G. G. M., 1992, ApJ, 401, 269

Chihara, H., Koike, C., Tsuchiyama, A., 2001, PASJ, 53, 243

Chihara, H., Koike, C., Tsuchiyama, A., Tachibana, S., Sakamoto, D., 2002, A&A, 391, 267

Cook, D. J., Schlemmer, S., Balucani, N., et al., 1998, JPC A, 102, 1465

Crovisier, J., Leech, K., Bockelee-Morvan, D., et al., 1997, Sci, 275, 1904

Dartois, E., d'Hendecourt, L., Boulanger, F., et al., 1998, A&A, 331, 651

Dartois, E., Demyk, K., d'Hendecourt, L., & Ehrenfreund, P., 1999a, A&A, 351, 1066

Dartois, E., Schutte, W., Geballe, T. R., et al., 1999b, A&A, 342, L32

Dartois, E., Demyk, K., Gerin, M., & d'Hendecourt, L., 1999c, in Les Houches Ser. 11, Solid Interstellar Matter: The ISO Revolution, ed. L. d'Hendecourt , C. Joblin & A. Jones, EDP Sciences, Les Ulis, 161

Dartois, E., Gerin, M., & d'Hendecourt, L., 2000, A&A, 361, 1095

Demyk, K., Jones, A. P., Dartois, E., Cox, P., & d'Hendecourt, L., 1999, A&A, 349, 267

Demyk, K., Carrez, Ph., Leroux, H., et al., 2001, A&A, 368, L38

Ehrenfreund, P., Boogert, A. C. A., Gerakines, P. A., Tielens, A. G. G. M., & van Dishoeck, E. F., 1997, A&A, 328, 649

Ehrenfreund, P., Dartois, E., Demyk, K., & d'Hendecourt, L., 1998, A&A, 339, L17

Ehrenfreund, P., 1999, in Les Houches Ser. 11, Solid Interstellar Matter: The ISO Revolution, ed. L. d'Hendecourt , C. Joblin & A. Jones, EDP Sciences, Les Ulis, 231

Fabian, D., Henning, Th., Jäger, C., et al., 2001, A&A, 378, 228

Frenklach, M. & Feigelson, E. D., 1989, ApJ, 341, 372

de Graauw, T., Haser, L. N., Beintema, D. A., et al., 1996, A&A, 315, L49

Gerakines, P. A., Whittet, D. C. B., Ehrenfreund, P., et al., 1999, ApJ, 522, 357

d' Hendecourt, L. B., Allamandola, L. J., Grim, R. J. A., & Greenberg, J. M., 1986, A&A, 158, 119

d'Hendecourt, L., Jourdain de Muizon, M., Dartois, E., et al., 1996, A&A, 315, L365

d'Hendecourt, L., Joblin, C., & Jones, A., 1999 in Les Houches Ser. 11, Solid Interstellar Matter: The ISO Revolution, EDP Sciences, Les Ulis

Henning, T. & Mutschke, H., 1997, A&A, 327, 743

Hiraoka, K., Miyagoshi, T., Takayama, T., Yamamoto, K., & Kihara, Y., 1998, ApJ, 498, 710

Hiraoka, K., Sato, T., Sato, S., et al., 2002, ApJ, 577, 265

Jäger, C., Molster, F. J., Dorschner, J., et al., 1998, A&A, 339, 904

Joblin, C., Abergel, A., Bregman, J., et al., 2000, in ESA Pub. Ser. ESA-SP 456, ISO beyond the peaks: The 2nd ISO workshop on analytical spectroscopy, eds. A. Salama, M. F. Kessler, K. Leech & B. Schulz., 49

Joblin, C., Toublanc, D., Boissel, P., & Tielens, A.G.G.M., 2002, Mol. Phys., in press

Kemper, F., Waters, L. B. F. M., de Koter, A., & Tielens, A. G. G. M., 2001, A&A, 369, 132

Kemper, F., de Koter, A., Waters, L. B. F. M., Bouwman, J., & Tielens, A. G. G. M., 2002, A&A, 384, 585

Koike, C., Shibai, H., & Tuchiyama, A., 1993, MNRAS, 264, 654

Koike, C., Tsuchiyama, A., Shibai, H., et al., 2000, A&A, 363, 1115

Kwok, S., Volk, K., & Hrivnak, B. J., 1999, A&A, 350, L35

Léger, A. & Puget, J.-L., 1984, A&A, 137, L5

Li, A., Draine, B. T., 2001, ApJ, 554, 778

Malfait, K., Waelkens, C., Waters, L. B. F. M., et al., 1998, A&A, 332, L25

Meeus, G., Waters, L. B. F. M., Bouwman, J., et al., 2001, A&A, 365, 476

Molster, F. J., Lim, T. L., Sylvester, R. J., et al., 2001a, A&A, 372, 165

Molster, F. J., Yamamura, I., Waters, L. B. F., et al., 2001b, A&A, 366, 923

Molster, F. J., Waters, L. B. F. M., Tielens, A. G. G. M., & Barlow, M. J., 2002a, A&A, 382, 184

Molster, F. J., Waters, L. B. F. M., & Tielens, A. G. G. M., 2002b, A&A, 382, 222

Molster, F. J., Waters, L. B. F. M., Tielens, A. G. G. M., Koike, C., & Chihara, H., 2002c, A&A, 382, 241

Moutou, C., Léger, A., & d'Hendecourt, L., 1996, A&A, 310, 297

Moutou, C., Verstraete, L., Léger, A., Sellgren, K., & Schmidt, W., 2000, A&A 354, L17

Nummelin, A., Whittet, D. C. B., Gibb, E. L., Gerakines, P. A., & Chiar, J. E., 2001, ApJ, 558, 185

Pech, C., Joblin, C., & Boissel, P., 2002, A&A 388, 639

Peeters, E., Hony, S., Van Kerckhoven, C., et al., 2002, A&A, 390, 1089

Roelfsema, P. R., Cox, P., Tielens, A. G. G. M., et al., 1996, A&A, 315, L289

Sylvester, R. J., Kemper, F., Barlow, M. J., et al., 1999, A&A, 352, 587

Tielens, A. G. G. M. & Hagen, W., 1982, A&A, 114, 245

Tielens, A. G. G. M., Waters, L. B. F. M., Molster, F. J., & Justtanont, K., 1998, Ap&SS, 255, 415

Tsuchiyama, A., 1998, Min. J., 20, 59

Van Kerckhoven, C., Hony, S., & Peeters, E., et al., 2000, A&A, 357, 1013

Verstraete, L., Pech, C., Moutou, C., et al., 2001, A&A, 372, 981

Waelkens, C., Waters, L. B. F. M., de Graauw, M. S., et al., 1996, A&A, 315, L245

Waters, L. B. F. M., Molster, F. J., de Jong, T., et al., 1996, A&A, 315, L361

Waters, L. B. F. M., Beintema, D. A., Zijlstra, A. A., et al., 1998a, A&A, 331, L61

Waters, L. B. F. M., Cami, J., de Jong, T., et al., 1998b, Nat, 391, 868

Zhitnikov, R. A. & Dmitriev, Yu. A., 2002, A&A, 386, 1129

AN ATLAS OF FULL-GRATING SHORT WAVELENGTH SPECTROMETER SPECTRA: CLASSIFICATION AND PROCESSING

Kathleen E. Kraemer[1], **Steve D. Price**[1], **Gregory C. Sloan**[2,3], **Helen J. Walker**[4], and **Russell F. Shipman**[5]

[1] Air Force Research Laboratory, Space Vehicles Directorate, 29 Randolph Road, Hanscom AFB, MA 01731, USA
[2] Institute for Scientific Research, Boston College, Chestnut Hill, MA 02467, USA
[3] Infrared Spectrograph Science Center, Cornell University, Ithaca, NY 14853-6801, USA
[4] Rutherford Appleton Laboratory, Chilton, Didcot, Oxon, OX11 0QX, UK
[5] SRON, PO Box 800, 9700 AV Groningen, The Netherlands

ABSTRACT

The Infrared Space Observatory (ISO) took almost 1250 2.4–45.2 μm spectra of over 900 celestial objects with the Short Wavelength Spectrometer in full-grating mode. Based on these data, we have developed a comprehensive system of infrared spectral classification. The primary discriminant between the classes is the temperature of the dominant emitter, e.g. a hot stellar photosphere or a cold dust cloud. Subgroups are made up of objects with similar spectral features, such as silicate absorption or atomic fine-structure lines. We have also created an atlas of uniformly processed spectra from these data. Starting from the most processed form available from the ISO Data Archive, which consists of 288 spectral segments per observation, we have reduced and combined these data into single, continuous spectra. The classifications, atlas, and processing software have been submitted for publication in the Astrophysical Journal Supplement and will also be available to the general astronomical community upon request.

Key words: ISO – SWS

1. BACKGROUND

Spectral classification is the process of placing objects into groups based on the characteristics of their spectral energy distributions (SEDs). From this process, we can learn about the physical properties of both the specific objects and about the general class of objects to which they belong. The utility and robustness of a particular classification scheme depends on the wavelength region observed, the spectral resolution and sensitivity of the instrument used, as well as on the number of objects and the range of object types observed. The experimental objective of the STARTYPE project was to use the superior abilities of the Infrared Space Observatory (ISO) to develop infrared classification schemes more detailed and sophisticated than previous works such as those derived from the Infrared Astrophysical Satellite (IRAS) Low Resolution Spectrometer (LRS) and to create an atlas of the spectra.

With these goals in mind, we began with the the moderate-resolution full-grating spectra from the Short Wavelength Spectrometer (SWS), observing mode S01. In this mode, the full spectral range of SWS, 2.4–45 μm, was observed at spectral resolutions of $\sim$500–2500, and features as faint as a few Janskys could be detected. In the process of classifying the spectra, the need was recognized for processing of the data beyond the pipeline-produced Auto-Analysis Results (AAR) and before the atlas could be created. The classifications of the SWS spectra are described in Section 2, the post-pipeline processing is described in Section 3, and Section 4 summarizes our results and future plans.

2. CLASSIFICATION

The classification began with the browse products from the Off-Line Processing (OLP) version 7.1. These are postcard-sized plots of each of the 1248 SWS full-grating spectra. Three levels of classification were envisioned for the SWS spectra, based on 1) the temperature of the dominant emitter; 2) the dominant spectral feature; and 3) spectral details. The browse products were suitable for the first two levels of classification in $\sim$75% of the spectra; the rest required the development of additional processing methods (Section 3) before they could be properly classified. The third level of classification, in which the fine details of the spectral features are examined, was deferred to the future. Examples of this level of classification include the work of Heras et al. (2002) which examine the sequence of normal stars, and the work being done with the oxygen-rich dust features in the 10–20 μm range (e. g. Sloan et al. 2001, Posch et al. 2002).

2.1. THE CLASSIFICATIONS

The spectra were sorted independently by K. Kraemer and by G. Sloan. Six temperature groups were created, plus a seventh group containing problem spectra. The groups are:

1. Stars with only photospheric emission. All objects in this group have optical classifications.
2. Stars with photospheric emission, but also noticeable dust emission, typically around 10 μm. These are usually asymptotic giant branch (AGB) stars or red supergiants.
3. Warm, dusty objects. These have little or no photospheric emission, and their SEDs peak between $\sim$5 and $\sim$20 μm. Most are AGB stars, planetary nebulae (PNe), or transition objects.
4. Cool, dusty objects. Cool dust dominates the emission in these objects, with their SEDs peaking longword of 20 μm but still within the SWS spectral range. Most of the objects

are evolved stars, but some are young stellar objects or H II regions.

5. Very red objects. The SEDs of these objects are still rising at 45 μm, the end of the SWS spectral range. Most are star forming regions or PNe.

6. Emission lines but no continuum. These spectra have no continuum emission in the SWS range but do show emission from atomic and ionic fine-structure lines. The objects in this group include supernova remnants and novae.

7. Flux-free and/or fatally flawed spectra. These spectra were either too faint or had instrumental problems which made them impossible to classify. Roughly 15% of the SWS full-grating spectra are in this category.
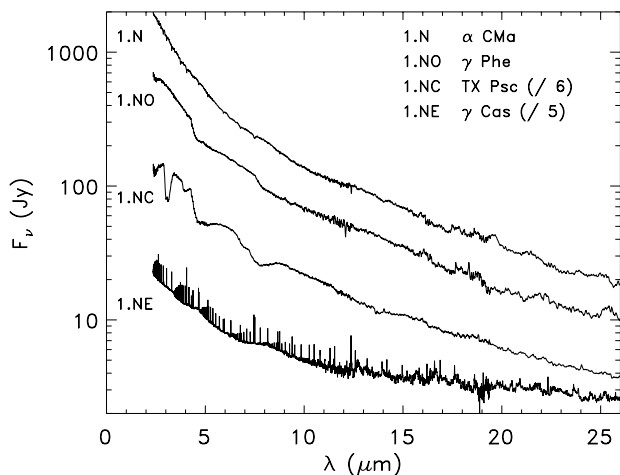

Figure 1. Sample spectra from the naked star class, Group 1.

Twenty-three feature-based subgroups were created, described in Table 1, although not all subgroups appear in all temperature groups. Groups containing oxygen-rich dust features include subgroups SA, SE, SB, SEC, and SC. Those with carbon-rich features include CE, CR, CT, and CN. Subgroups with nebular emission include PN, PU, U, UE, and E. Combinations of subgroups are also possible: C/SE, C/SC, and U/SC; other subgroups are W, F, and M. Additional properties of a spectrum may be indicated by the presence of one or more suffixes: e (emission lines), u (UIR features), p (peculiar), g (extragalatic), w (wrong coordinates), f (flagged by the pipeline), and : or :: (noisy). For example, NGC 6537 is classified as a 5.PNup, which indicates that its SED is very red (5), the most prominent spectral features are highly ionized emission lines (PN), UIR features are present but not strong (u), there is something unusual in the spectrum (p), which, in this case, is the presence of crystalline silicates.

Kraemer et al. (2002) present the complete classifications for all 1248 S01 spectra, as well as more detailed descriptions of the feature subgroups. Fig. 1 shows examples of Group 1 spectra, and Fig. 2 shows examples of carbon-rich subgroups.
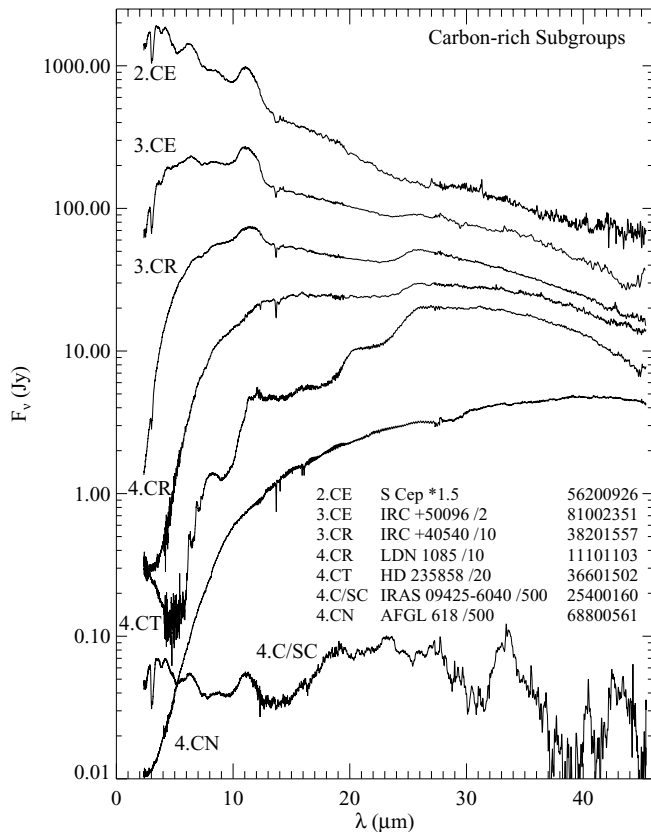

Figure 2. Sample spectra from the subgroups with carbon-rich dust.

2.2. COMPARISON WITH LRS SPECTRA

The IRAS LRS observed roughly 50% of the SWS objects. We compared our classifications to three LRS-based schemes: the initial LRS classes (IRAS Science Team, 1986; IRAS Explanatory Supplement, 1988), the AutoClass algorithm (Cheeseman et al. 1989), and the work by Kwok, Volk, & Bidelman (1997). Generally, the systems agreed well for most broad categories of objects: $\sim 90\%$ of naked stars, $\sim 90\%$ of silicate emission sources, $\sim 80\%$ of silicate absorption sources, and $\sim 80\%$ of carbon-rich sources. Some discrepancies did occur. Most can be attributed to the limited spectral range, spectral resolution, and sensitivity of the LRS, which are then reflected in the various classification systems. Examples of sources with the same LRS class which were distinguished in our scheme are shown in Fig. 3.

3. POST-PIPELINE PROCESSING

In addition to the infrared spectral classification described above, one of the goals of the STARTYPE project was to produce an atlas of mid-infrared spectra. Ideally, the spectra should be as uniform as possible, reproducible by anyone starting with the same data, and readily available for use by the community. While the browse products were sufficient for most of the classifications, problems such as discontinuities at band edges and

Table 1. Classification Subgroups

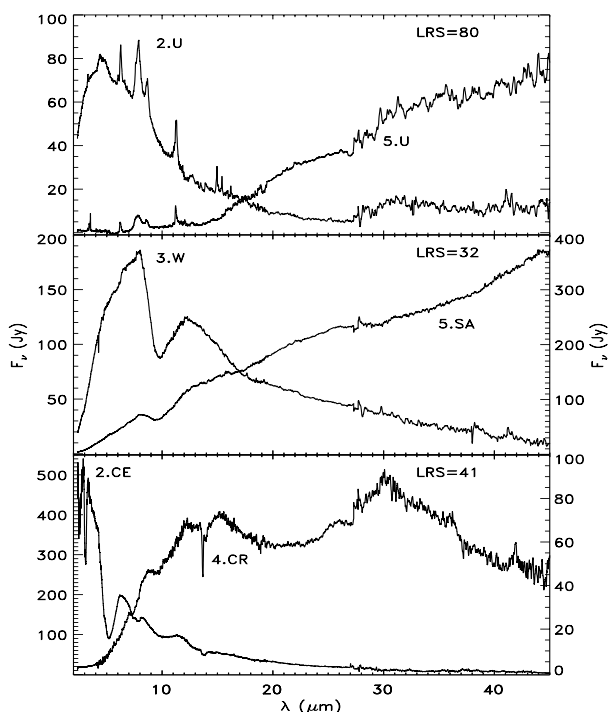| Subgroup	Description
N	Stellar photospheric emission with no dust, H lines in absorption, if present
NE	Photospheric emission with H lines in emission
NO	Photospheric emission with Oxygen-rich (e.g. SiO, CO, OH) molecular bands
NC	Photospheric emission with Carbon-rich (e.g. CO, C_2H_2) molecular bands
SE	O-rich dust emission from amorphous silicates (10–12 & 18–20 μm)
SB	self-absorbed silicate emission (10 μm)
SA	Silicate absorption (10 μm)
SC	Emission from crystalline silicate grains ($\sim$33, 40, 43 μm)
SEC	Crystalline silicates including the 11 μm feature
CE	C-rich dust emission (11.5 μm)
CR	C-rich dust with a redder continuum, 11.5 & 26 μm emission features, 13.7 μm absorption
CT	C-rich dust, 8, 11.5, 21, & 26 μm emission features, no 13.7 μm absorption feature
CN	C-rich proto-planetary nebulae
C/SE	C-rich photospheric emission plus 10 μm silicate emission
C/SC	C-rich plus crystalline silicates past $\sim$30 μm
U	Unidentified infrared (UIR) features, usually associated with polycyclic aromatic hydrocarbons (PAHs)
E	Atomic and ionic fine-structure emission lines (e.g. [Ne II], [S IV], [Ar II])
UE	UIRs plus fine-structure emission lines
U/SC	UIRs plus crystalline silicates past $\sim$30 μm
PN	High ionization emission lines from planetary nebulae (e.g. Fe II, Ar V, Mg V)
PU	PNe with UIR features
W	Wolf-Rayet stars, SEDs peak $\sim$6–8 μm
F	Featureless
M	Miscellaneous

Figure 3. Comparison of objects with the same LRS class but distinct SWS spectra. Top: LRS = 80 (UIR emission); HR 4049 (2.U) and HD 97048 (5.U) (smoothed). Middle: LRS = 32 (blue SED plus silicate absorption); WR 112 (3.W) and V645 Cyg (5.SA). Bottom: LRS = 41 (C-rich); RY Dra (2.CE) and IRAS 22303+5950 (4.CR).

glitches necessitated further processing of the data before the creation of the atlas. For this, we started with the "basic science" product from the ISO Data Archive, the AAR.

For the SWS, the AAR data consist of 12 spectral bands, with 12 detectors in each band, each of which was scanned up and down in wavelength, for a total of 288 discrete spectra for each observation. Four scanning and sampling rates were available, so any given observation could have one of four spectral resolutions and sensitivities. Our processing rectifies the 288 spectral segments into single spectra in as uniform a manner as possible, given the different observing configurations available to an observer and the variation in the SEDs of the sources observed. To do so, several steps were performed on every spectrum. Details appear in Sloan et al. (2002), while the general steps are outlined below.

For each spectral band, a low resolution median was created. Each detector within the band, in each scan direction, was flat-fielded to the median. The detectors and scans were correlated for spike rejection. Thus, glitches, which typically occur in single detectors or in only one scan direction, were rejected, while emission lines, which should appear in most detectors in both directions, were retained. The data were re-sampled onto a uniform wavelength grid, the spacing of which depended on the speed at which an observation was made. Starting with either the 3.5–4.0 μm band or the 26.5–29.5 μm band, depending on which contained more flux, each band was normalized to its neighbors using data in the overlap regions between the bands. The overlapping data were then trimmed, leaving a sin-

gle, continuous spectrum for each observation. Fig. 4 shows a comparison of the AAR data to our final product for two sample objects. Fig. 5 compares the current browse products to our spectra for three more objects.
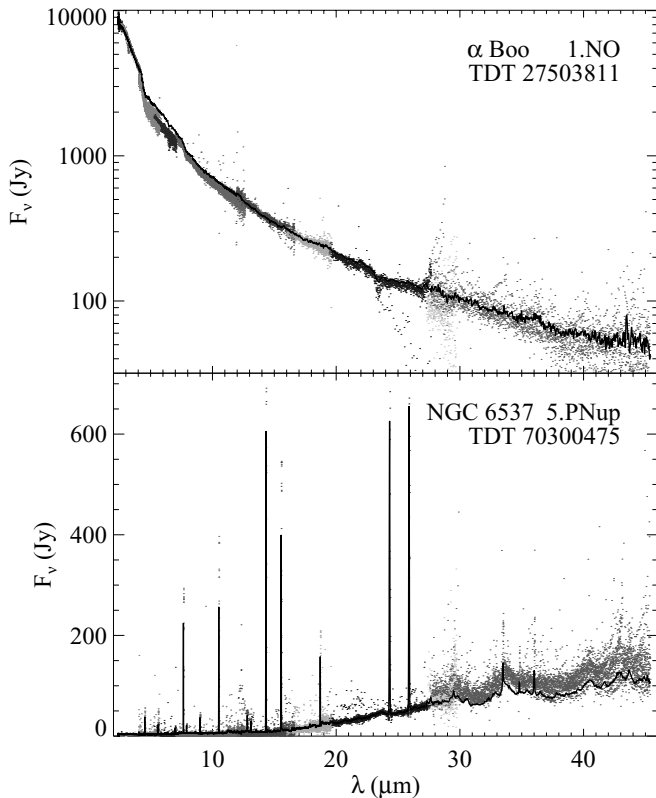

Figure 4. Comparison of the AAR data (dots) with our final spectra (solid line). Top: α Boo; bottom: NGC 6537. The different shades of gray are used for the different spectral bands of SWS.
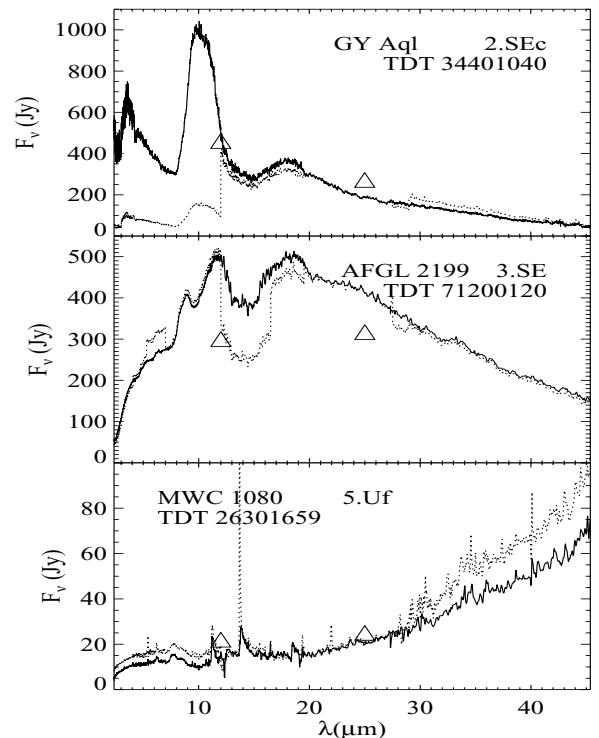

Figure 5. Comparison of our processing results (solid line) with the browse product (dotted line) and IRAS photometry (triangles) for three representative spectra. The top and center panels (GY Aql and AFGL 2199, respectively) illustrate how our normalization process removes discontinuities which can disguise the true nature of a spectrum for a blue and red source respectively. The bottom panel (MWC 1080) shows how our spike rejection removes most of a strong spurious feature at 13.5 μm which appears in the browse product. Our algorithm also rejects several other spikes flagged by ISO which appear in the browse data (e.g. at 5.4, 19.3, and 22 μm).

4. SUMMARY

We have examined and categorized all 1248 SWS S01 full-grating spectra into a comprehensive system of infrared classifications. The primary groupings are based on the temperature of the strongest emitter, while the subgroups are based on prominent spectral features. The spectra have been processed and renormalized in a uniform manner. Our processing produces a single, continuous spectrum from the 288 spectral segments provided in the AAR file. The classifications are available in Kraemer et al. (2002). The atlas of spectra, and the software used to produce it (Sloan et al. 2002), will be available through the ISO Data Archive and upon request from the authors. The next step in this project is to extend the classification and processing effort to the other spectroscopic datasets from ISO: high spectral resolution SWS (S06) observations (Kraemer et al. in preparation), post-cryogen SWS observations (Price et al. in preparation), PHT-S 2.5–11.5 μm spectra (∼1600 observations, Hodge et al. in preparation), and the CAM CVF spectra (Engelke et al. in preparation).

REFERENCES

Cheeseman, P., Stutz, J., Self, M., Taylor, W., Goebel, J., Volk, K., & Walker, H. 1989 "Automatic Classification of Spectra from the Infrared Astronomical Satellite" (NASA RP-1217) (Washington: GPO)

IRAS Catalogs & Atlases, Vol. I: Explanatory Supplement 1988, (Washington:NASA)

IRAS Science Team 1986, AAS, 65, 607

Heras, A. M., Shipman, R. F., Price, S. D., et al. 2002, A & A, submitted

Kraemer, K. E., Sloan, G. C., Price, S. D., & Walker, H. J. 2002, ApJS, 140, 389

Kwok, S., Volk, K, & Bidelman, W. P. 1997, ApJS, 112, 557

Posch, T. 2002, this volume

Sloan, G. C., Goebel, J. H., Kraemer, K. E., & Price, S. D. 2001, BAAS, 199, 92.04

Sloan, G. C., Kraemer, K. E., Price, S. D., & Shipman, R. F., 2002, ApJS, submitted

IR SPECTROSCOPY OF CARBON NANOPARTICLES FROM LASER-INDUCED GAS PYROLYSIS

Isabel Llamas Jansa, Harald Mutschke, Dominik Clément, Cornelia Jäger, and Thomas Henning

Astrophysical Institute and University Observatory, Friedrich Schiller University Jena, Germany

ABSTRACT

Because amorphous carbon grains are considered among the main components of cosmic dust, the characterization of their physical and chemical properties in the laboratory is needed to explain the data obtained by the astronomical observations. Material produced by laser pyrolysis of acetylene in the laboratory has been analyzed in the 4000-500 cm^{-1} (2.5-20 μm) region of the infrared spectrum. It is believed that this material serves as analogue to the cosmic dust. The obtained spectra have been compared to IRAS and ISO infrared spectroscopic data.

Key words: Infrared:stars - Dust,extinction - Circumstellar matter - methods:laboratory

1. ASTROPHYSICAL BACKGROUND

In the last years different carbon dust analogues have been proposed as candidates to interpret the family of unidentified infrared bands (UIBs) observed in different cosmic environments (Pendleton & Allamandola 2002). Coals and irradiated ices are some among them. Solid particles of hydrogenated amorphous carbon with sizes from nm to μm have become a good analogue for solid carbon in space. Carbon atoms appear in the last stages of the evolution of low and intermediate mass stars in a process in which the fusion of three helium nuclei results in the formation of a carbon nucleus. During the asymptotic giant branch (AGB) phase of the stellar evolution the material from the center of the star is dredged up to the surface, and in later stages, it is ejected as part of the stellar wind. At the final stage the star (white dwarf) produces UV photons and the circumstellar envelope suffers from ionization becoming a planetary nebula (PN). Observational spectra of the AGB and PN phases show strong differences between them. Laboratory and observational efforts have been done to resolve this issue.

2. PARTICLE PRODUCTION

Nano-sized carbon grains (soot), as an analogue material, is produced here by the Laser Pyrolysis method which is close to the mechanism postulated for carbon dust formation in the envelopes of evolved C-rich stars. Super-saturated vapor is generated by decomposition of acetylene (C_2H_2) as precursor gas. A pulsed CO_2 laser, with a wavelength of approximately 10 μm, is used to deliver energy for the pyrolysis, and lowered background pressure in the expansion chamber is maintained in order to extend the condensation zone of the soot particles. Helium is used as buffer gas.

Acetylene must be photosensized by addition of sulfurhexafluorite (SF_6) in different amounts in order to achieve the dissociation of the molecules. The ratio between SF_6 and C_2H_2 flow rates is expected to be responsible for the temperature of the reaction flame (Herlin et al. 1998; Schnaiter et al. 1999) together with the total gas flow. The gas flow velocity and the volume occupied by the gas mixture during the reaction are used to calculate the residence time of the particles in the reaction zone. The physical properties of the resulting powders can be controlled by changing the synthesis parameters (see Tab. 1). We have studied in detail their influence on the material's properties.

Table 1. Experimental parameters and calculated residence time of the samples.

Ratio SF_6/C_2H_2	Pressure (Torr)	Laser power (mJ/pulse)	Residence time (ms)
30/30	360	40.0	1.89
30/70	360	41.0	1.37
30/90	360	40.0	0.95
30/150	360	35.5	0.63

The produced particles are extracted into a free jet and deposited on a KBr substrate under vacuum conditions. In-situ IR spectroscopy of the carbon layer is carried out by means of an FTIR spectrometer coupled to the laser pyrolysis setup. Also, a portion of the carbon material is collected on a filter situated in the exhaust line of the flow reactor and is embedded in KBr pellets for conventional IR transmission spectroscopy, for comparison. Samples for TEM structural analysis are taken directly from the beam.

3. PARTICLE STRUCTURE

Samples for electron microscopy have been prepared by placing a copper grid, supporting a "lacey carbon" film, in the particle beam. The HRTEM image (Fig. 1) shows that the particles
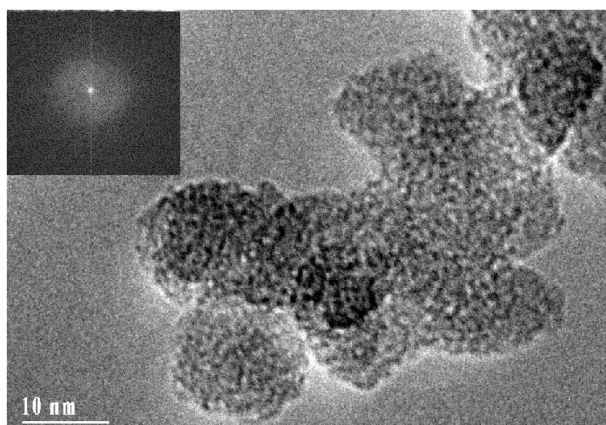
Figure 1. TEM and Electron diffraction images of carbon black particles produced by laser pyrolysis of acetylene. The material looks structurally amorphous.

are of nearly spherical shape with a diameter of about 10 nm. No graphite-like crystallites or BSUs (basic structural units) are observed within the primary particles, which means that they are either too small (in a- and c- direction) or too much disturbed to be resolved. Thus, the grains look structurally amorphous as it is also confirmed by the electron diffraction pattern (see image included in Fig. 1).

4. SPECTROSCOPIC RESULTS

The absorption spectra of carbon nanoparticles produced by laser pyrolysis of acetylene have been measured in the infrared (IR) region by using the KBr pellet technique. The vibrational bands, corresponding to the different functional groups, are superimposed over the continuum absorption. In Fig. 2, showing the trend related to the SF_6/C_2H_2 ratio, the continuum has been removed and the curves have been shifted for clarity. The first group of bands corresponds to the C-H stretching vibrations between 2700 and 3200 cm^{-1} (3.2 and 3.6 μm). In this region, four strong features, attributed to aliphatic functional groups, appear over the continuum. The low CH_3/CH_2 ratio present in these spectra indicates the growth of long saturated aliphatic hydrocarbon chains [-($CH_2)_n$-CH_3]. A weak aromatic =C-H stretching band at 3048 cm^{-1} (3.28 μm) is also evident. This feature is strongest in the sample produced at high C_2H_2 content (30:150), which is related to a short residence time in the reaction zone (see Tab. 1). The strong aliphatic bands relative to the aromatic feature at 3.3 μm resemble more these from the early stages of evolution from the AGB to the PN phase (Kwok et al. 1999).

The IR range between 5 and 15 μm displays a variety of features (Fig. 2 and Tab. 2). A strong peak around 1613 cm^{-1} (6.20 μm) is assigned to the C=C group vibration. This vibration appears when the medium-range structure of the aromatic structural units within the particles is strongly disturbed, for example, by the incorporation of hydrogen (Jäger et al. 1999). A broad band, centered at 3600 cm^{-1} (2.78 μm, not shown
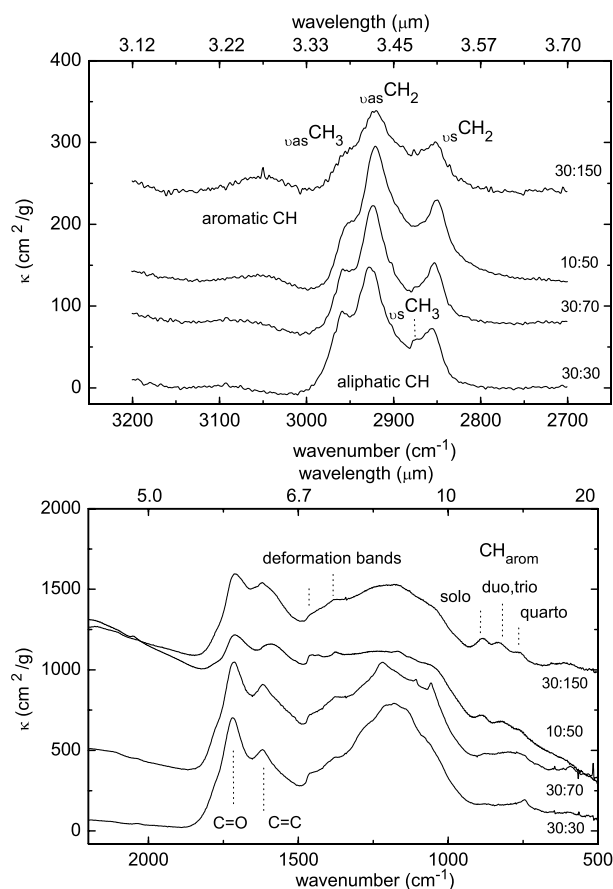

Figure 2. Infrared spectra measured in KBr pellets showing the vibrational features of the pyrolysis products synthesized at different SF_6/C_2H_2 ratios in the precursor gas mixture. The curves have been shifted for clarity

in Fig. 2), is visible in the spectra and can be attributed to O-H stretching vibrations. These OH groups were implemented during the KBr pellet production. The related OH deformation band between 1640 and 1610 cm^{-1} can blend with the C=C stretching band. Therefore, the assignment of this feature is not unique.

The more acetylene in the precursor mixture, the less hydrogen is incorporated for C-H bonding. This is also evidenced by the weakening of the -CH_3 deformation bands around 1463 cm^{-1} (6.8 μm) and 1378 cm^{-1} (7.3 μm). The carbonyl C=O stretching vibration appears at around 1700 cm^{-1} (5.85 μm). The oxygen content of the samples is proven by the presence of this strong feature. The intensity of the band rapidly increased with the exposure of the sample to air. In between 1420 and 1100 cm^{-1} (7 and 9 μm) a composite massive is observed. It is composed of a variety of vibrations such as C-H aliphatic deformations, C-O-C vibrations, C=C deformations and C-C stretching vibrations.

Three bands due to aromatic C-H out-of-plane vibrations are present between 900 and 660 cm^{-1} (11 and 15 μm). They are clearly recognizable in the sample produced at a ratio of 30:150. The features at 890 cm^{-1} (11.23 μm, solo), at 826

Table 2. Vibrational frequencies of the principal features observed in the IR range between 5 and 15 μm and their implications.

Vibrating Groups	Wavenumber (cm^{-1})	Wavelength (μm)	Remarks
Aromatic C=C stretching	1613	6.20	needs structural disorder
C=O stretch	1724	5.80	contamination
CH$_3$, CH$_2$ deformation bands	1463	6.8	hint to aliphatic
	1378	7.3	structures
C-H aliphatic and aromatic deformations, C-O-C vibrations, C=C deformations, C-C bands	1420-1100	7-9	no structural information
Aromatic C-H out-of-	890	11.23, solo	
plane vibrations	826	12.10,duo/trio	information about arom.
	745	13.43,quarto	condensation

cm^{-1} (12.10 μm, duo, trio) and at 745 cm^{-1} (13.43 μm, quarto) can be attributed to one, two or more H atoms bonded to an aromatic ring. The behaviour of these features corresponds quite well to the behaviour of the aromatic C-H stretching band. Our experiments demonstrate that the decrease of the C$_2$H$_2$ content in the precursor mixture reduces the content of aromatic C-H stretching bonds.

5. COMPARISON OF EXPERIMENTAL METHODS

The comparison of conventional spectra of C powder embedded in a KBr pellet with in-situ measurements shows the discrepancies between these two methods of measure. There is lower CH$_3$ content in the case of KBr-pellet measurements evidenced in the lack of the CH$_3$ vibrations either in the stretching band or in the deformation bands around 1460 and 1380 cm^{-1} (6.8 and 7.2 μm). Also evident is the difference in the content of oxygen, as shown by the stronger carbonyl (C=O) vibration in the pellet measurement (Fig. 3). The pronounced band at 1560 cm^{-1} observed in the in-situ measurement, can be tentatively attributed to the C=C stretching vibrations. The broadening and the shift of the C=C stretching vibration in the KBr pellet measurement supports our assumption that the band at 1613 cm^{-1} (6.20 μm) is a blend of two different groups. From these results we conclude that in situ spectroscopy of carbon samples is highly preferable compared to KBr pellet measurements in order to avoid contamination of the surface.

6. ASTRONOMICAL IMPLICATIONS

The astrophysical relevance of our laser-pyrolysis produced material can be observed in Figs. 4 and 5. These are comparisons between samples obtained in laboratory and PPNe spectra measured by IRAS and ISO SWS01. The complete agreement with the observed IRAS 05341+0852 spectrum (Joblin et al. 1996) is not achieved although the main part of the CH stretching band is well fitted. The strength of the 2870 cm^{-1} (3.48 μm) band, assigned to the CH$_3$ symmetric stretching vibrations, in-
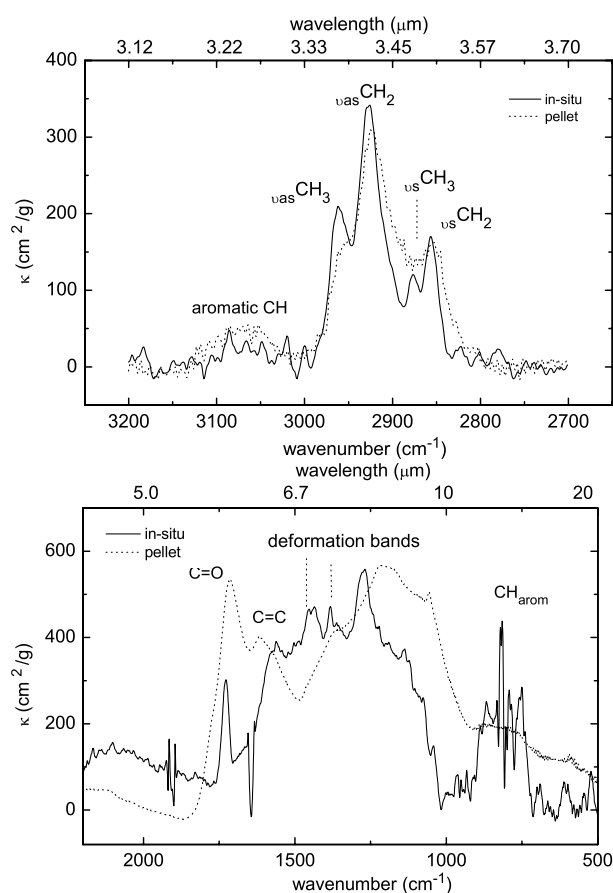

Figure 3. Comparison between pellet (dotted) and in-situ (solid) measurements for the material produced at SF$_6$/C$_2$H$_2$=30:70.

dicates shorter chains in the observed material. The main discrepancy, however, comes from the strong intensity difference between the 3030 cm^{-1} (3.3 μm) aromatic CH stretching band relative to that of the 2941 cm^{-1} (3.4 μm) aliphatic band. This corresponds to a higher hydrogen containing aromatic material present in proto-planetary nebulae. Fig. 5 shows a detailed

72

comparison of the 2500-500 cm^{-1} (4-20 μm) spectral range. The agreement with the PPNe IRAS 22272+5435 spectrum (Kwok et al. 2001) in this range is quite satisfactory, particularly in the case of the deformation band at 1460 cm^{-1} (6.8 μm) and the aromatic C=C stretching band at around 1600 cm^{-1} (6.2 μm). In the case of the IRAS 07134+1005 PPNe (Kwok et al. 1999) (see Fig. 5) the agreement between the laboratory and the observed spectra in the range between 900 and 700 cm^{-1} (11-14 μm) is remarkable. The observed bands at 11.3, 12.1, 12.4, and 13.3 μm belong to the characteristic features of proto-planetary nebulae (Kwok et al. 1999).
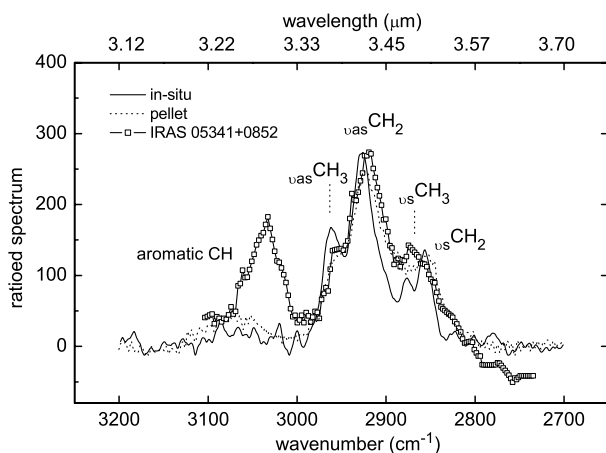

Figure 4. Comparison of the C-H stretching bands of a produced material with IRAS data of the PPNe IRAS 05341+0852 (squares).
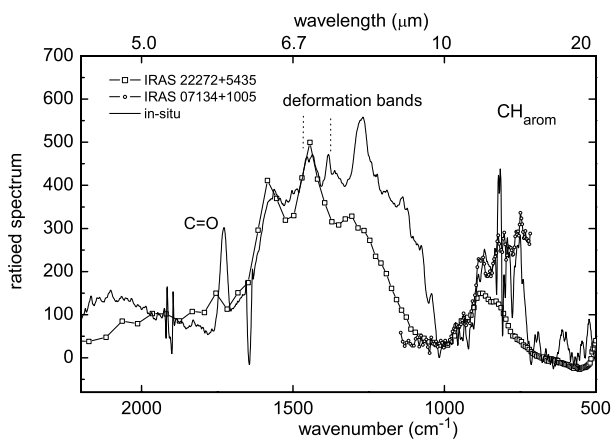

Figure 5. Comparison of the in-situ mid-infrared spectrum of a produced material with the ISO SWS01 data (*) of the PPNe IRAS 22272+5435 (squares) and IRAS 07134+1005 (circles).

served weakening of the aliphatic C-H vibrational bands (3.4 and 6.9 μm) and the increase of the aromatic 3.3 and 6.2 μm features in PNe (Kwok et al. 1999). The different properties of dust in these stages are still not resolved. Dust formed in the outflows of evolved stars suffers from UV irradiation which leads to dehydrogenation and aromatization of carbon structures. Furthermore, re-condensation processes can contribute to develop the zoo of different carbon dust species. However, despite the good fitting with the astronomical data of some of the features, one has to take into account that the CH bands are present in a large variety of hydrogenated carbon-based materials. Thus, IR spectroscopy is not a complete tool for the global identification of the carriers of the dust features. Other analysis such as UV and FUV measurements and TEM images have also to be carried out for the complete characterization of the carrier, since it is known that the spectral structure of the hydrogenated carbonaceous material is closely related to the electronic structure in the material and the arrangement of the BSUs within it.

REFERENCES

Herlin N., Bohn I., Reynaud C., Cauchetier M., Galvez A., and Rouzaud J. N., 1998, A&A, 330, 1127
Jäger C., Henning Th., Schlögl R., and Spillecke O., 1999, Journal of Non-Crystalline Solids, 258, 161
Joblin C.,Tielens A., Allamandolla L.J., and Geballe T.,1996, ApJ,458,610 2001, A&A, 597, 607
Kwok S., Volk K., and Hrivnak B.J., 1999, A&A, 350, L35
Kwok S., Volk K., and Bernath P., 2001, ApJ, 554, L87
Pendleton Y.J., and Allamandola L.J., 2002, A&ASS, 138, 75
Schnaiter M., Henning Th., Mutschke H., Kohn B., Ehbrecht M., and Huisken F., 1999, ApJ, 519, 687

7. CONCLUSIONS

It is known that dehydrogenation and aromatization occur between the PPNe and PNe phases. This is evidenced by the ob-